

**3D LASER IMAGING OF TEKTITES.** C. Fry<sup>1</sup>, C. Samson<sup>1</sup>, S. Butler<sup>2</sup>, P.J.A. McCausland<sup>3</sup>, and R.K. Herd<sup>1,4</sup>,  
<sup>1</sup>Dept. of Earth Sciences, Carleton U., Ottawa, ON, Canada K1S 5B6; cfry2@connect.carleton.ca, <sup>2</sup>Dept. of Geological Sciences, U. of Saskatchewan, Saskatoon, SK, Canada S7N 5E2, <sup>3</sup>Dept. of Earth Sciences, Western U., London, ON, Canada N6A 5B7, <sup>4</sup>Earth Sciences Sector, Natural Resources Canada, Ottawa, ON, Canada K1A 0E8.

**Introduction and objectives:** Tektites are glassy objects that form mostly from molten silicate host rock during a meteorite impact. Tektites develop distinctive shapes that are related to their motion upon cooling while airborne.

In this study, eight tektites were imaged using a laser camera. The use of high-resolution 3D laser imaging has been demonstrated for terrestrial hand samples, and stony<sup>[1,2,3]</sup> and iron<sup>[4]</sup> meteorites over the past few years. Adjacent images with a small amount of overlap were aligned and gradually assembled into 3D models. These models are volumetrically accurate, allowing for the density to be calculated<sup>[1,2,3]</sup>. The results are comparable to those found using the Archimedean bead method<sup>[1,2]</sup>. The models can also serve as archival records.

The objectives of the study were: (1) to test if 3D laser imaging is applicable to tektites, given their glassy nature, (2) to demonstrate the capability of the laser camera to capture classic surface features of tektites such as vesicles and schlieren lines, (3) to derive densities from the 3D models, and (4) to compute rotational parameters for future flow simulation investigations (Table 1).

**Samples and methods:** Eight splash-form tektites from the Australasian strewn field, exhibiting a variety of shapes and surface features, were imaged using a Konica-Minolta Vivid 9i non-contact laser camera at a distance of  $\approx 0.7$  m and a resolution of 640 x 480 voxels. Each tektite was rotated at increments of 20° on a turntable, in three separate orientations. At least 52 individual images were taken to provide a comprehensive coverage of the surface of each sample. On average, 18 images were combined to create a complete 3D model of each tektite (Figs 1, 2, 3). The volume can be calculated from the image and the mean density calculated. Our calculated densities range between 2.20 and 2.60 g/cm<sup>3</sup>, in rough accord with early measurements of the densities of Australasian tektites<sup>[5]</sup>. Chapman et al. (1964) found that tektite density was more strongly influenced by chemical composition than gas bubbles.

**Challenges of imaging tektites:** The glassy nature of tektites did not pose a challenge to laser imaging. The laser beam did not penetrate the samples and captured surface features with a high

fidelity. This might be due to the fact that the surfaces of the tektites studied were opaque.

Assembling 3D models of tektites proved to be laborious. The first difficulty is related to their fairly rounded surfaces. The lack of salient features implied that the alignment program had difficulty linking adjacent images correctly in place, even when the operator manually seeded the software with corresponding points on both images. For this reason, the ball-shape tektites were the most difficult to model. The second difficulty is the vesicular nature of several tektite surfaces. In most cases, the presence of vesicles produces a hole in the point cloud as the cavity does not reflect the projected laser beam. Extensive manual editing was required to fill these holes.

**Portrait gallery:** Fig. 1 presents a dumbbell tektite exhibiting a number of large and distinctive depressions (the surface transitions from smooth to pockmarked with shallow vesicles) that provided reference points to easily assemble the model.

Fig. 2 shows a model of a disc tektite. Distinct surficial features such as large vesicles and a cleft, are clearly visible, but more subtle ones, like schlieren lines, are lost. Schlieren lines are probably picked up by the human eye because of their dark-light linear intensity pattern rather than by any associated surficial ripples.

Fig. 3 is a tektite with a unique shape, featuring a large concavity.

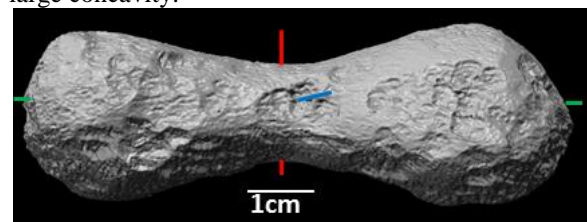


Fig. 1: Dumbbell Tektite TB1

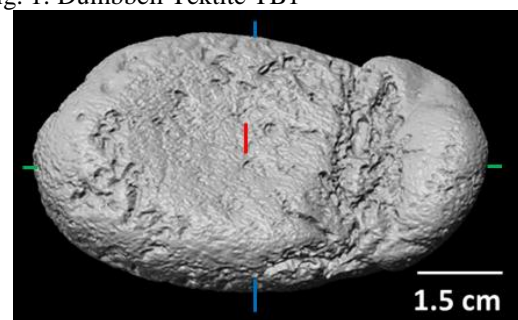


Fig. 2: Disc tektite TD2.

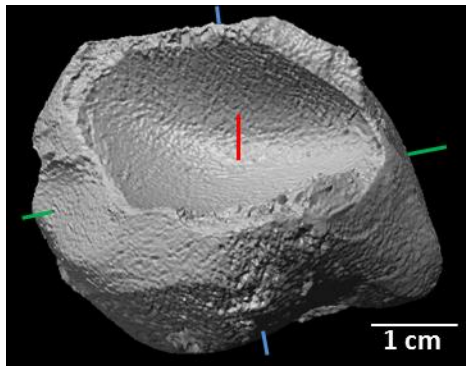


Fig. 3. Tektite TU1 exhibiting a unique shape.

**Inertia and rotation period:** The inertia tensor for the tektites was calculated from the 3D models. Assuming uniform density, the centre of mass of each model was located and the principal moments of inertia for rotation around orthogonal axes through the centre of mass (displayed in red, blue and green in Figs 1, 2, 3) were calculated and listed in increasing order ( $I_1 < I_2 < I_3$ ) (Table 1). In order to perform the volume integrals required to determine the coordinates of the centre of mass and the moments of inertia, the divergence theorem was used to transform to surface integrals over the known surface. As well as constraining the rotation rate, the moments of inertia represent the second moment of the mass distribution and therefore serve as first order shape descriptors.

For instance, the teardrop and dumbbells all have  $I_1 \ll I_2 \sim I_3$  which is indicative of prolate objects. TD1 and TD2 are both triaxial and as a result have three different moments of inertia. TU1 is of similar length in all directions (Fig. 3). As a result, its three moments are similar in magnitude.

Centrifugal forces that result from rotation cause mass to move away from the rotation axis and hence increase the moment of inertia about this axis while the tektites are hot enough to viscously deform. As a result, it is likely that the eigenvector corresponding to the largest moment of inertia (red) corresponds to the rotation axis of the tektite while in flight. Furthermore, there are constraints on the angular momentum needed in order for a rotating fluid blob to achieve a given shape<sup>[6]</sup>. Using this approach, the rotation period for the tektites was found to be of the order of 1s (Table 1). The rotation rate can only be estimated for tektites that do not show signs of having separated or broken while brittle or in the late stages of their viscous deformation

**Future work:** We have demonstrated that 3D laser imaging of the surfaces of the splash-form tektites is possible with resolution sufficient to image surface bubble pits but not schlieren. These images will have further use as image processing techniques can be used to study surface textures and their possible relationship to the overall shapes of the tektites. Also, these images can be imported into simulation software to develop a better understanding of the deformation of tektites while in flight.

**Acknowledgements:** We thank Dr. Mel Stauffer for the loan of the tektites used in this study.

**References:** [1] McCausland et al. (2011) *Meteoritics & Planet. Sci.* 46, 1097-1109. [2] Fry, C. et al. (2011) *LPSC XLII*, Abstract #1427. [3] Smith et al. (2006) *JGR*, doi:10.1029/2005JE00262. [4] Fry et al. (2012) *LPSC XLIII*, Abstract #2703. [5] Chapman et al. (1964) *Geochem. Cosmo. Acta.* 28, 821-839 [6] Butler et al. (2011) *J. Fluid Mech.* 667, 358-368.

Sample	Mass [g]	Shape	Volume [cm <sup>3</sup> ]	Density [cm <sup>3</sup> /g]	Moments of inertia [kg.m <sup>2</sup> ]			Rotation period [s]
					I <sub>1</sub>	I <sub>2</sub>	I <sub>3</sub>	
TT1	175.00	Teardrop	72.02	2.43	3.09E-05	8.74E-05	8.96E-05	
TT2	71.53	Teardrop	30.12	2.38	5.64E-06	2.59E-05	2.69E-05	
TT4	21.20	Teardrop	8.79	2.41	7.78E-07	3.50E-06	3.56E-06	
TO3	59.67	Oblong ball	27.18	2.20	6.95E-06	9.27E-06	1.06E-05	0.66
TB1	72.69	Dumbbell	28.97	2.51	4.74E-06	4.47E-05	4.49E-05	0.98
TD1	150.00	Disc	57.73	2.60	2.60E-05	6.86E-05	8.50E-05	1.16
TD2	84.27	Disc	33.73	2.50	1.23E-05	3.15E-05	4.13E-05	0.74
TU1	102.60	Unique	43.02	2.38	2.52E-05	3.16E-05	3.96E-05	

Table 1: Tektite density and rotational parameters